Desalination and Water Treatment
www.deswater.com

doi: 10.5004/dwt.2017.20532

70 (2017) 330–338
April

An analysis of the sensitivity of fixed bed adsorption for diazinon removal: experimental and modeling studies

H. Esfandian[a,*], B. Khoshandam[a,*], M. Parvini[a], A. Samadi-Maybodi[b]

[a]*Faculty of Chemical Engineering, Gas and Petroleum, Semnan University, Semnan, Iran, emails: Hossein.Esfandian@gmail.com (H. Esfandian), bkhoshandam@semnan.ac.ir (B. Khoshandam), m.parvini@ semnan.ac.ir (M. Parvini)*
[b]*Analytical Division, Faculty of Chemistry, University of Mazandaran, Babolsar, Iran, email: samadi@umz.ac.ir*

Received 30 August 2016; Accepted 19 January 2017

ABSTRACT

In this paper, a novel microcrystalline sodalite was synthesized. In addition, the structural characterization of this zeolite was done using the X-Ray Fluorescence (XRF), X-ray diffraction, scanning electron microscope (SEM), and Fourier Transform Infrared Spectroscopy (FTIR) analyses. Cu_2O nanoparticles (30–60 nm) were loaded on the zeolite and utilized as an adsorbent to remove diazinon in fixed bed column. The SEM energy-dispersive X-ray of modified zeolite shows that the amount of copper loading on the zeolite was equal to 4.5 wt%. The thermodynamic parameters ΔH, ΔS, and ΔG were evaluated in batch system. Thermodynamic parameters indicated that the sorption of diazinon onto zeolite was feasible, spontaneous, and exothermic under studied conditions. The effect of bed depth (5–15 cm), initial concentration (50, 75, and 100 mg/L), and flow rate (0.5, 1, and 1.5 mL/min), as important variable parameters, was investigated on the column performance. Given the external mass transfer resistance and the axial dispersion with non-linear isotherm, a general model was used to predict the breakthrough curves of the fixed bed for diazinon sorption. The numerical calculation of the model equations was done by the Computational Fluid Dynamics (CFD) software. There was a good agreement between the experimental data and the predicted theoretical breakthrough curves.

Keywords: Diazinon; Zeolite; Fixed bed column; Breakthrough curve; CFD software

1. Introduction

At present, one of the important concerns about environmental pollution is the existence of pesticide in soils, groundwater, and surface water. This is because there are numerous hazardous compounds in the structure of pesticides that are harmful for both the environment and human health [1]. In many agricultural areas, the organophosphate pesticides are considered as examples of insecticides that have widespread application in pest control. In addition, different sources such as agricultural drainage [2], wastewater treatment plants [3], and other water resources yield these pesticides. Pesticides are considered as a primarily non-biodegradable environmental pollution that are chiefly carcinogenic. Toxicity of pesticides and their post-degradation products will seriously increase the levels of pollution in both water and the environment. Hence, they have become most noticeable throughout the world [4].

Diazinon, a kind of organophosphate pesticide, is used as a control measure for pests in fruits, vegetables, and field crops. However, excessive concentration of this insecticide is harmful to organisms and blood. Therefore, the application rate should be meticulously determined on the chance that the toxicant brings contamination to groundwater or seawater [5,6]. However, diazinon absorption into skin can easily occur. Also, it can show the same characteristic with other toxins such as pyrethrins [7]. The maximum permitted concentration

* Corresponding author.

of 0.5 μg/L has been determined by European Union for all pesticides in drinking water [8]. To remove the toxicant from water, several different treatment processes were used, such as the adsorption processes [9,10], advanced oxidation processes [11,12], and electrocoagulation process [6]. One of the most effective methods to remove pollutants from the environment is the adsorption method. In this method, an equipment is used that is easy to use and readily available. However, the sorption method is not energy consuming. Also, treatment using this method is cost effective [13–17]. To eliminate diazinon from water and wastewater, several sorbents such as agricultural soil [18], surfactant modified agricultural soil [19], organozeolites [20], and modified bentonite [21] were used.

Over the last 35 years, zeolites have been successfully employed in the chemical industry and environmental protection based on their significant physical and chemical properties including cation exchange, molecular sieving, and adsorbing capability [22]. Zeolites fall into a desirable class of advanced crystalline microporous inorganic materials with amazing properties, which make them the best possible choice for applications such as the molecular sieving, shape-selective catalytic, and ion-exchange processes [23]. They have microporous channel systems with high surface areas. These properties are beneficial compared with the other classical support materials that are of special importance to the adsorbent [24,25]. Sodalite is regarded as one of the most typical artificial zeolites that is primarily a traditional zeolite mainly produced using the hydrothermal crystallization method [26]. Small pore size (2.8 Å) and considerable ion-exchange capacity are the main characteristics of this zeolite. Moreover, it has attracted great attention in industry and is utilized in applications such as optical material [27], hydrogen storage [28], and catalyst support [29].

Different researches investigated the application of sorbents for pesticides removal from aqueous solution and water. For example, the capacity of MCM-41 and MCM-48, as mesoporous silicas, was studied in the batch sorption process for adsorption of fenitothion and diazinon from non-polar solvent [30]. Atrazine, lindane, and diazinon were removed from water using the organzeolite as a low-cost sorbent. Accordingly, the impact of various operating parameters was scrutinized on the adsorption of diazinon, atrazine, and lindane onto organozeolite and isotherm of equilibrium that are related to the abovementioned adsorption process [20].

The aim of this research was synthesis of micro-sodalite zeolite with new procedure and its surface modification by copper oxide (Cu_2O). By modification of zeolite surface by copper oxide, the performance of the sorption process is significantly improved (copper oxide has high ability to form π-complex by sulfur in diazinon structure). The application of modified micro-sodalite in continues mode (fixed bed column) and study important parameters (bed height, flow rate, and initial concentration) on the diazinon removal process.As you know, The application of modified micro-sodalite in continues mode is too important. The effect of temperature on the removal of diazinon is also explored in batch adsorption experiments. In order to better understand the adsorption characteristic, thermodynamic models were employed to evaluate the sorption process. Also, the theoretical values were obtained from the solution of the mathematical model using the CFD software.

2. Experimental work and procedure

2.1. Reagents and chemicals

Diazinon pesticide with 95%–96% purity and copper oxide (Cu_2O) with a 30–60 nm particle size and the two formulations, namely sodium metasilicate ($Na_2O_3Si{\cdot}5H_2O$) and sodium aluminate ($NaAlO_2$), were purchased from Merck (Darmstadt, Germany). The solution pH was adjusted using H_2SO_4 (0.5 M) and NaOH (0.5 M). A UV–Vis spectrophotometer technique was used to specify the diazinon concentration. Spectra were recorded at maximum wavelengths (l max.) 247 nm [6,30].

2.2. Synthesis of micro-sodalite zeolite

In order to synthesize sodalite micro-zeolite, the hydrothermal crystallization method was employed using sodium metasilicate ($Na_2O_3Si{\cdot}5H_2O$) and sodium aluminate ($NaAlO_2$) as silica and aluminum sources, respectively. Using the standard synthesis, solution A was prepared by dissolving 8.924 g $Na_2O_3Si{\cdot}5H_2O$ (43% H_2O, 29% Na_2O, 28% SiO_2) in 15 mL of 2.36 M NaOH solution at 70°C. In addition, solution B was prepared through dissolving 0.341 g of $NaAlO_2$ in 5 mL of 2.36 M NaOH solution at 70°C. At the same time, solution A was mixed with solution B dropwise and was kept there for 72 h under stirring before it could finally reach hydrothermicity. After that, a Teflon-lined stainless-steel autoclave was used to heat produced gel at 100°C for 48 h. Centrifuge (5,000 rpm) was used at the end of the process to separate the sodalites. Double-distilled water was also used to wash the sodalite several times. After washing, sodalite dried overnight at 80°C.

2.3. Modification of sodalite zeolite by copper nanoparticles

Through the grains draining in a dispersed suspension of nanoparticles, nanoparticles loading on zeolite grains were carried out. To do so, 0.1 g of Cu_2O nanoparticles in the range of 30–60 nm was added into an Erlenmeyer flask containing 10 mL distilled water. The mixture in Erlenmeyer flask was sonicated for a few minutes to achieve a suspension with high uniformity. Subsequently, 2 g sodalite zeolite was spilled into the flasks and shook moderately for 2 h. At the end, the mixture in the flasks were dried at 80°C for 10 h. The loading rate of Cu_2O nanoparticles on the zeolite was 4.5 wt% [31,32].

2.4. Instrumentation

X-ray diffraction (XRD) patterns were investigated by a GBC MMA diffractometer using the Cu Kα radiation. Scans were recorded in an angular range from 5° to 70°. Scanning electron microscope (SEM) model S3400, Hitachi, Japan, was employed to examine the surface of the sodalite zeolite. Using gold and palladium to enhance the quality of the image, the sample was coated by a sputter coater with conductive materials. The density and thickness of coating were 30.00 nm and 19.32 g/cm^3, respectively. Energy-dispersive X-ray (EDX) spectra were recorded on an EDX Genesis XM2 attached to SEM. FTIR spectrometer (Shimadzu 4100) was used to obtain the sodalite infrared spectra. This was done in order to determine the sodalite functional groups. Spectra were collected

with a spectrometer using KBr pellets. In each case, the homogenization of 1.0 mg of dried sodalite and 100 mg of KBr was conducted with the aid of mortar and pestle. Later, they were pressed onto a transparent tablet at 200 kgf/cm^2 for 5 min. Characterization of pellets was done using an FTIR spectrometer in the transmittance (%) mode with a scan resolution of 4 cm^{-1} in the range 4,200–500 cm^{-1}.

2.5. Batch adsorption experiments

Batch adsorption experiments were performed using temperature as an important variable. The adsorption of diazinon on modified zeolite was conducted to study the effect of temperature parameter (at constant parameters such as pH, contact time, adsorbent dosage, and initial concentration), and determine the conditions that could lead to the maximum amount of diazinon removal.

2.6. Column experiments

Continuous-flow experiments for diazinon removal were done in a fixed bed column (columns were manufactured by glass) with an inner diameter and length of 10 and 20 cm, respectively. At the top and bottom of the column, a porous sheet (mesh 42) was attached. A uniform inlet flow of solution into the column was provided by glass beads with the height of 2 cm (1.5 mm in diameter), which was placed at the bottom of column. To achieve different bed heights, 4.6, 8.1, and 12.5 g of sorbents were added to give 5, 10, and 15 cm of height, respectively. The flow rate and concentration effect on diazinon sorption were investigated at 0.5, 1, and 1.5 mL/min and 50, 75, and 100 mg/L for a fixed bed depth of 5 cm, respectively. The desired flow rate of diazinon solution at the column was provided by a peristaltic pump (pp40, Miclins India). Samples collection was done at the effluent of the column. Later, samples were analyzed for diazinon concentration by a UV–Vis spectrophotometer. Each experiment was carried out in duplicate to obtain the reproducibility rate and the mean value used for each set of values. The experimental error was below 5%, and no significant differences were observed in the experiment results.

The total quantity of diazinon sorbed in the column (M_{ad}) is calculated from the area above the breakthrough curve (outlet diazinon concentration vs. time) multiplied by the flow rate (F) (Eq. (1)):

$$M_{ad} = FC_0 \int_0^{t_e} \left(1 - \frac{C_t}{C_0}\right) dt \tag{1}$$

Dividing the diazinon (M_{ad}) by the sorbent mass (M) leads to the uptake capacity (Q) of the modified zeolite. The total quantity of diazinon sent to the fixed bed column can be calculated from Eq. (2):

$$M_{total} = C_o.F.t_e \tag{2}$$

where C_o, t_e, and F are the inlet diazinon concentration (mg/L), the exhaustion time (min), and the volumetric flow rate (mL/min), respectively. Total removal of diazinon (%) can be presented as the ratio of diazinon mass adsorbed (M_{ad}) to the total amount of diazinon sent to the column (M_{total}) as Eq. (3):

$$\text{Total diazinon removal \%} = \frac{M_{ad}}{M_{total}} \times 100 \tag{3}$$

2.7. Mathematical model

The CFD simulation with its fixed bed reactor packed with porous spherical particles was used to solve sets of ordinary and/or partial differential equations similar to the one used for modeling, predicting, and optimizing the performance of water treatment processes, sorption operations, aquifer flow behavior, etc. Using the finite element method, the numerical solution was obtained by the CFD model. It depends on the mass, momentum, and energy conservation equations of the system, which is made up of diazinon, a modified zeolite bed, and tank walls. The finite element analysis accompanied by adaptive meshing and error control is run by the software with the aid of a series of numerical solvers. It is very important to follow six basic steps as explained earlier when the model in CFD approach is being set up. In the present research, the model was used to determine account axial dispersion, external mass transfer, interparticle diffusion, and non-linear adsorption isotherm [33,34]. The following model governs the equations for component i:

We can write the continuity equation in the bulk-fluid phase as [33,34]:

$$\frac{\partial C_{bi}}{\partial t} = -\upsilon \frac{\partial C_{bi}}{\partial z} + D_L \frac{\partial^2 C_{bi}}{\partial z^2} - \frac{(1-\varepsilon_b)}{\varepsilon_b} \rho_b \frac{\partial q_i}{\partial t} \tag{4}$$

With regard to the film diffusion, the sorption term $\frac{\partial_{qi}}{\partial t}$ can be written as follows:

$$\frac{\partial q_i}{\partial t} = \frac{3k_{fi}}{R_p \rho_p} (C_{bi} - C_{pi,R=R_p}) \tag{5}$$

To replace the film diffusion expression back into Eq. (4) and rearrange the results, the following equation is used:

$$-D_L \frac{\partial^2 C_{bi}}{\partial z^2} + \upsilon \frac{\partial C_{bi}}{\partial z} + \frac{\partial C_{bi}}{\partial t} + \frac{3k_{fi}(1-\varepsilon_p)}{R_p \rho_p} \left(C_{bi} - C_{pi,R=R_p}\right) = 0 \tag{6}$$

Continuity equation inside the macropores:

The intraparticle mass balance in the radial direction explains the pore diffusion, which is expressed by the following equation in spherical coordinates:

$$\varepsilon_p \frac{\partial C_{pi}}{\partial t} + \left(1-\varepsilon_p\right) \rho_p \frac{\partial q_i}{\partial t} - \varepsilon_p D_{pi} \left[\frac{1}{R_p^2} \frac{\partial}{\partial R} \left(R^2 \frac{\partial C_{pi}}{\partial R}\right)\right] = 0 \tag{7}$$

Initial and boundary conditions:

$$C_{bi} = C_{bi}\left(0, z\right) = 0 \tag{8}$$

$$C_{pi} = C_{pi}\left(0, R, z\right) = 0 \tag{9}$$

$$Z = 0 : \frac{\partial C_{bi}}{\partial z} = \frac{\upsilon}{D_L}(C_{bi} - C_{oi}) \quad (10)$$

$$Z = L : \frac{\partial C_{bi}}{\partial z} = 0 \quad (11)$$

$$R = 0 : \frac{\partial C_{pi}}{\partial R} = 0 \quad (12)$$

$$R = R_p : \frac{\partial C_{pi}}{\partial R} = \frac{k_{fi}}{\varepsilon_p D_{pi}}(C_{bi} - C_{pi,R=R_p}) \quad (13)$$

The three elements in this equation, namely the scaled bulk concentration, c_{bi}, scaled intraparticle concentration, c_{pi}, and scaled particle dimension, are expressed as mentioned earlier: $c_{bi} = C_{bi}/C_{oi}$, $c_{pi} = C_{pi}/C_{oi}$, $r = R/R_p$.

The component Langmuir isotherm model eased the calculation of the concentration inside spherical particle C_{pi} [28,29]:

$$q_i = \frac{q_{mi} b_i C_{oi} c_{pi}}{1 + b_j C_{0i} c_{pj}} \quad (14)$$

and regarding the following relation:

$$\frac{\partial q_i}{\partial t} = \frac{\partial q_i}{\partial c_{pi}} \cdot \frac{\partial c_{pi}}{\partial t} \quad (15)$$

where:

$$\frac{\partial q_i}{\partial c_{pi}} = \frac{q_{mi} b_i (1 + b_j C_{0i} c_{pj})}{\left(1 + b_j C_{0i} c_{pj}\right)^2} \quad (16)$$

We can restate the model Eqs. (6) and (7) into the following semi-dimensionless equations:

$$-D_L \frac{\partial^2 c_{bi}}{\partial z^2} + \upsilon \frac{\partial c_{bi}}{\partial z} + \frac{\partial C_{bi}}{\partial t} + \frac{3k_{fi}(1-\varepsilon_p)}{R_p \rho_p}\left(c_{bi} - c_{pi,R=R_p}\right) = 0 \quad (17)$$

$$\left[\varepsilon_p + (1-\varepsilon_p)\rho_p \frac{\partial q_i}{\partial c_{pi}}\right]\frac{\partial c_{pi}}{\partial t} = \frac{\varepsilon_p D_{pi}}{R_p^2}\frac{\partial^2 c_{pi}}{\partial r^2} + \frac{2\varepsilon_p D_{pi}}{R_p^2 r}\frac{\partial c_{pi}}{\partial r} \quad (18)$$

Initial and boundary conditions turn into:

$$c_{bi} = c_{bi}(0, z) = 0 \quad (19)$$

$$c_{pi} = c_{pi}(0, R, z) = 0 \quad (20)$$

$$z = 0 : \frac{\partial c_{bi}}{\partial z} = \frac{\upsilon}{D_L}(c_{bi} - c_{oi}) \quad (21)$$

$$z = L : \frac{\partial c_{bi}}{\partial z} = 0 \quad (22)$$

$$r = 0 : \frac{\partial c_{pi}}{\partial r} = 0 \quad (23)$$

$$r = 1 : \frac{\partial c_{pi}}{\partial r} = \frac{R_p k_{fi}}{\varepsilon_p D_{pi}}(c_{bi} - c_{pi,R=R_p}) \quad (24)$$

On the assumption that diazinon molecules are larger than micro-sodalite pores, the only sorption phenomenon occurs on the zeolite surface. Therefore, we neglect the diffusion of poison particles into the pores of the adsorbent and only solve the equations related to the mass transfer around the column considering the adsorption term.

3. Results and discussion

3.1. Characterization of sodalite zeolite

The XRD, EDX, SEM, and FTIR were used to structural characterization of the sodalite zeolites. The XRD of sodalite and modified sodalite by Cu_2O nanoparticles are shown in Figs. 1(a) and (b). As can be seen in Fig. 1(a), the XRD shows the peaks at 2θ values of 14.1°, 20.1°, 22.4°, 24.5°, 27.7°, 31.9°, 34.9°, 37.9°, 43.1°, 45.7°, and 48.1°. They were all given by Treacy and Higgins [35], which showed a successful synthesis of micro-sodalite zeolite indicating a desirable crystallinity. The Cu-modified sodalite also showed good agreement with works carried out previously [26,28,36,37]. The crystalline phase SEM image helps create a useful technique to determine the crystals morphology and size. Fig. 2 shows the SEM image of a modified sodalite. As can be seen, the spherical micro-sized particle has been formed with an average size of 20 μm. Fig. 3 presents the elemental analysis of Cu-modified sodalite by means of EDX. The presence of Cu peaks in EDX spectrum was explained in detail, and the amounts of elements were given in Table 1. Fig. 4 shows the FTIR analysis of modified sodalite in the 600–4,200 cm^{-1} range. The peak located at 702 cm^{-1} matches the bond of Al–O fragment. In addition, the strong broad peak at 998.9 cm^{-1} is connected to the asymmetric stretching mode of the tetrahedrally coordinated Si [38,39]. The peak at 1,639 cm^{-1} is the result of the free water bending vibration. The strong broad band at 3,400–3,700 cm^{-1} (centered at 3,467 cm^{-1}) is attributed to the stretching of hydroxyl group (OH–) of silicate lattice [40–42]. The appearance of a new absorption peak at 434 cm^{-1} is the result of the formation of single four-membered ring of sodalite unit [39].

3.2. Effect of temperature on adsorption of diazinon

The effect of temperature on the adsorption was investigated in the temperature range of 20°C–50°C at pH 6 and adsorbent dosage of 0.2 g into 100 mL (50 ppm) of solutions. The equilibrium contact time for adsorption was maintained at 20 min. The results indicate that the percentage of adsorption decreases with every increase in temperature from 20°C to 50°C. This implies that the adsorption process is exothermic in nature. The effect of temperature on the removal efficiency is shown in Table 2. Results of Table 2 were used for determination of changes in Gibbs free energy (Δ*G*), heat of adsorption (Δ*H*), and entropy (Δ*S*) of the diazinon sorption from aqueous solutions.

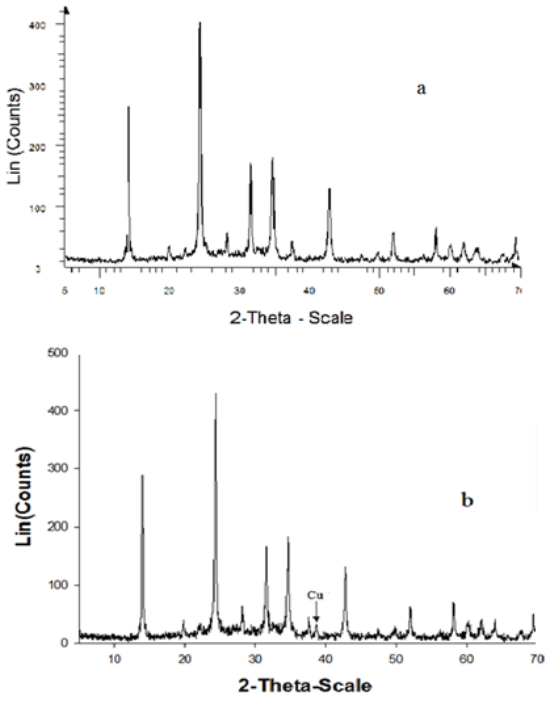

Fig. 1. X-ray diffraction of synthesized sodalite zeolite: (a) sodalite and (b) Cu-modified sodalite.

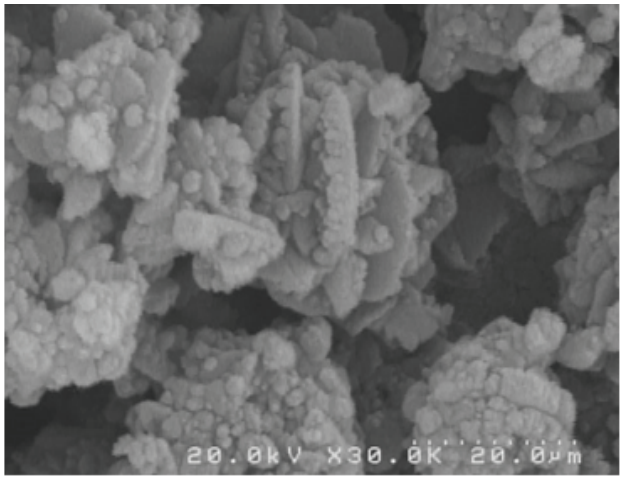

Fig. 2. Scanning electron micrographs of sodalite zeolite.

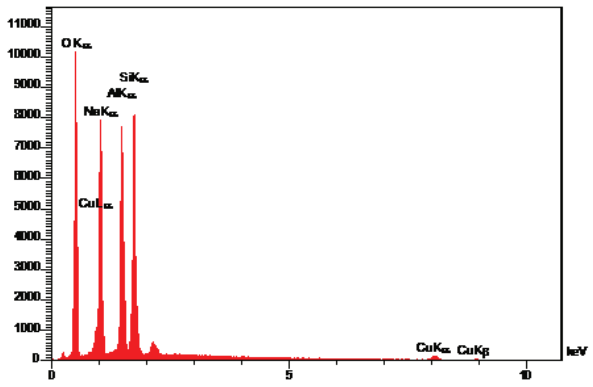

Fig. 3. The EDX spectrum for copper-modified sodalite.

Table 1
Amounts of the elements obtained by EDX analysis

Element	Wt%
O	49.13
Na	17.07
Al	14.55
Si	14.75
Cu	4.5

3.2.1. Effect of temperature on thermodynamics parameter on adsorption of diazinon

The variation in the extent of sorption with respect to temperature has been explained based on thermodynamic parameters. Various thermodynamic parameters such as enthalpy change ΔH, free energy change ΔG, and entropy change ΔS were calculated using Eqs. (25)–(27). The values of these parameters are presented in Table 3. Thermodynamic parameters ΔH, ΔS, and ΔG were calculated using the following equations:

$$K_c = \frac{F_e}{1 - F_e} \tag{25}$$

$$\log K_c = \frac{-\Delta H}{2.303RT} + \frac{\Delta S}{2.303R} \tag{26}$$

$$\Delta G = -RT \ln K_c \tag{27}$$

where F_e is the fraction of diazinon sorbed at equilibrium. The values of these parameters summarized in Table 3 showed that the enthalpy change ΔH is negative (exothermic) due to the decrease in adsorption on successive increase in temperature. The negative ΔG values showed the thermodynamically feasible and spontaneous nature of the sorption. The positive value of ΔS reveals the increased randomness at the solid–solution interface during the fixation of the diazinon on the active sites of the sorbent.

3.3. Simulation parameters

The parameters for diazinon adsorption modeling are presented in Table 4. The correlation of Chung and Wen [43] was used to determine the axial dispersion coefficient D_{Li} in a fixed bed column:

$$D_L = \frac{\mathrm{Re}}{(0.2 + 0.011 * \mathrm{Re}^{0.48})} \left(\frac{\mu_w}{\rho_w} \right) \tag{28}$$

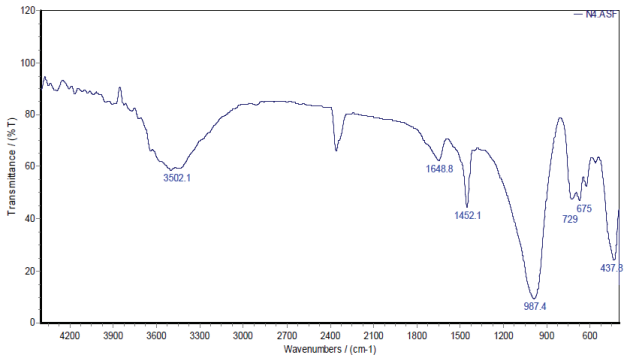

Fig. 4. FTIR spectrum of sodalite zeolite.

Table 2
The effect of temperature on the removal efficiency

Temperature (°C)	Removal efficiency of diazinon (%)
20	95.32
30	91.2
40	85.33
50	77.44

Liquid film mass transfer coefficient for each component was obtained using the correlation of Wilson and Geankoplis [44]:

$$Sh_i = \frac{1.09}{\varepsilon_p}\mathrm{Re}^{1/3} SC_i^{1/3} \quad \text{for} \quad 0.0015 < \mathrm{Re} < 55 \tag{29}$$

The value of liquid diffusivity coefficient (D_m) was obtained by means of the following equation [45]:

$$Dm_i = 2.74 \times 10^{-9} (MW_i)^{-1/3} \tag{30}$$

Eq. (31) was used to calculate the mean absolute percentage deviation (%Error) experimental data:

$$\%\mathrm{Error} = \frac{100}{\mathrm{ndat}} \sum_{i=1}^{\mathrm{ndat}} \left| \frac{\theta_{i,\mathrm{exp}} - \theta_{i,\mathrm{calc}}}{\theta_{i,\mathrm{exp}}} \right| \tag{31}$$

3.4. Effect of flow rate

One of the most important parameters during the evaluation of adsorbents performance in fixed bed column is the effect of the flow rate [46]. To evaluate the flow rate effect on the column performance, different flow rate (0.5, 1 and 1.5 mL/min) was used; the initial diazinon concentration and bed height were also constant at 5 cm and 50 mg/L, respectively. The experimental and predicted breakthrough curves at different flow rates for the effluent diazinon concentration vs. time are shown in Fig. 5. As can be seen, the predicted data can be fitted well with the experimental breakthrough data. Fig. 5 shows that the diazinon uptake was very rapid at lower flow because of more availability of reaction sites to sorb diazinon from aqueous solution. In the next step of process, because of gradual occupancy of the sites, the diazinon uptake from aqueous solution reduces. Increasing the flow rate will decrease the adsorbed diazinon. Also, the break point time decreases, and the steeper breakthrough curve is observed. Another point should be made that is by increasing the flow rate, solute does not have enough residence time to reach the adsorption equilibrium; therefore, the diazinon solution without occurrence of equilibrium leaves the column [47,48]. Table 5 shows sorption capacities, maximum diazinon sorption, or removal efficiency with regard to the flow rate. It was found that the total sorbed diazinon quantity, maximum diazinon sorption, and the values related to the percentage removal of diazinon declined with every increase in flow rate.

Table 3
Thermodynamic parameter for adsorption of diazinon onto zeolite

ΔH (kJ/mol)	ΔS (kJ/mol K)	T (°C)	ΔG (kJ/mol)	R^2
–1,059.8	3.253	20	–7.342	0.91
		30	–5.891	
		40	–4.582	
		50	–3.312	

Table 4
Adsorption modeling parameters

Pollutant	Diazinon
Particle diameter (d_p)	20 μm
Bed diameter (d_b)	2 cm
Bed porosity	0.37
Langmuir model (q_m)	61.32 mg/g
D_m (m²/s)	0.41×10^{-9}
$M_{w(\mathrm{Diazinon})}$	304.35 g/mol

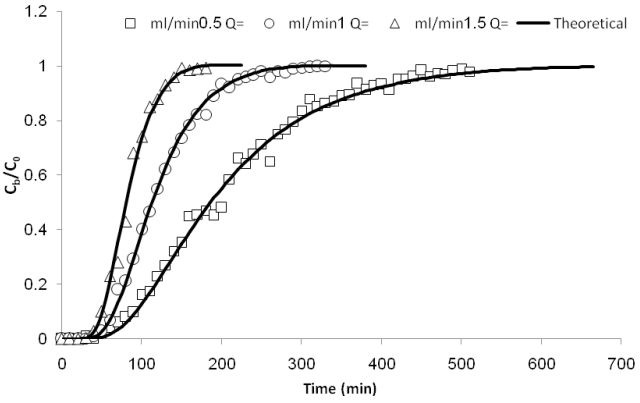

Fig. 5. Breakthrough curves for diazinon sorption onto modified zeolite at different flow rate.

Table 5
Column data and parameters obtained at different flow rates

Flow rate (mL/min)	t_b (min)	t_e (min)	M_{total} (mg)	M_{ad} (mg)	q (μg/g)	Removal efficiency (%)	%Error
0.5	100	370	9.25	4.86	1,080	52.54	4.38
1	70	200	10.00	4.78	1,062	47.8	3.18
1.5	50	140	10.5	4.5	1,000	42.86	4.75

3.5. Effect of initial diazinon concentration

The effect of initial diazinon concentration (50, 75 and 100 mg/L) on the sorption of diazinon by modified zeolite at fixed bed column can be seen in Fig. 6. The constant values of 5 cm and 0.5 mL/min were used for bed height and flow rate, respectively. It was found that the trend of the fitted curve agrees well with the experimental breakthrough data. As can be seen in Fig. 6, the breakthrough curves becomes much steeper upon any increase in the initial concentration because the increase in the solute concentration in the solution causes an increase in the driving force in favor of mass transfer. Thus, the diazinon ion in the solution will exchange faster with ion attached to the modified zeolite, and this situation will lead to the rapid exhaustion of zeolite. The adsorption data (sorption capacities, maximum diazinon sorption, or removal efficiency) were presented in Table 6. It was found that the decrease in the breakthrough and exhaustion time is caused by any increase in the initial concentration of diazinon from 50 to 100 mg/L.

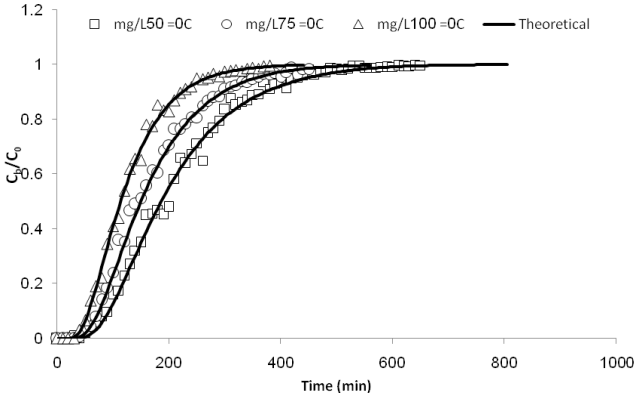

Fig. 6. Breakthrough curves for diazinon sorption onto modified zeolite at different initial concentration.

3.6. Effect of bed height

The adsorbent quantity in the fixed bed column has considerable effect on the diazinon uptake. The effect of changing bed height (from 5 to 15 cm) in fixed bed column onto diazinon removal from aqueous solution by modified are presented in Fig. 7. These experiments had been performed at 0.5 mL/min flow rate and 50 mg/L of initial diazinon concentration. Fig. 7 shows that the increase in the bed height from 5 to 15 cm leads to an increase in the treated solution volume ($V_{eff} = F \times t_e$).

In general, increasing the bed height provides enough time for the solute to adsorb into sorbent mass, and therefore, it stays more into the column and treats more volume of the wastewater. It was found that the increase in bed height leads to an increase in the adsorption capacity and removal efficiency of diazinon by modified zeolite. The maximum uptake of 1,820 μg/g for diazinon was observed at the maximum bed depth, namely 15 cm. The diazinon uptake increases with the bed height caused by the increase in the adsorbent quantities in the beds with more height. The more adsorbent quantity provides more adsorption sites for the diazinon binding. Furthermore, the bed height increases from 5 to 15 cm leading to an increase in the breakthrough time. This is simply due to the fact that the solute resides more in the column with the more availability of the adsorption sites [46,47]. In different bed heights, the diazinon uptake capacity with the modified zeolite remained almost constant (Table 7). Because the uptake capacity probably has a strong dependence on the amount of sorbent available for the adsorption [46]. As can be seen in Table 5, an increase in breakthrough time (t_b), exhaustion time (t_e), and removal efficiency due to the increase in bed height are observed. As seen in Fig. 7, there is a good agreement between the experimental and predicted values.

4. Conclusions

The new method used to synthesize micro-sodalite zeolite crystals was investigated in this paper. Results suggested that synthesis of this zeolite was performed successfully. To modify zeolite for removal of diazinon from water, Cu_2O nanoparticles were loaded on the surface of zeolite. Here depending on thiophenic sulfur compounds (i.e., diazinon) form either π-complexes using delocalized electrons of the aromatic ring or a direct S–M (i.e., sulfur group of diazinon and cupper) bond using the lone pair of electrons of the sulfur atom present in the plane of the ring. Thermodynamic studies demonstrate negative ΔG and ΔH, and positive ΔS. Results showed the exothermic nature of the adsorption. The effect of bed depth, initial diazinon concentration, and flow rate on the performance of fixed bed column for removal of diazinon by modified zeolite was investigated. It was found that the operating parameters have some effect on the breakthrough behavior of single component systems in packed bed column. Subsequently, it was realized that the breakpoint increases with bed height and decreases with feed flow rate and initial diazinon concentration. A general model was utilized to describe the transport and adsorption phenomena of the diazinon fixed bed adsorption column. The prediction models were validated with experimental breakthrough curves. The CFD prediction can be used for analyzing the experimental study of the sorption process in a packed bed.

Table 6
Column data and parameters obtained at different initial concentration

Initial concentration (mg/L)	t_b (min)	t_e (min)	M_{total} (mg)	M_{ad} (mg)	q (μg/g)	Removal efficiency (%)	%Error
50	100	370	9.25	4.86	1,080	52.54	4.38
75	80	290	10.87	4.9	1,100	45.08	3.17
100	60	230	11.5	5.04	1,120	43.83	2.55

Table 7
Column data and parameters obtained at different bed heights

Bed height (cm)	t_b (min)	t_e (min)	M_{total} (mg)	M_{ad} (mg)	q (μg/g)	Removal efficiency (%)	%Error
5	100	370	9.25	4.86	1,080	52.54	4.38
10	150	750	18.75	13.1	1,630	69.77	9.31
15	200	1,180	29.53	22.8	1,820	77.42	10.91

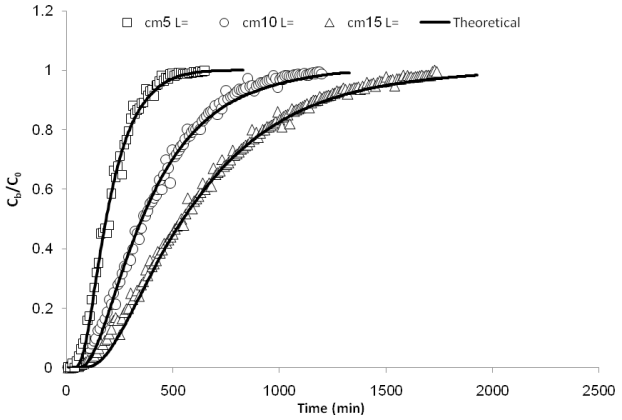

Fig. 7. Breakthrough curves for diazinon sorption onto modified zeolite at different bed heights.

Symbols

A — Cross-sectional area of the adsorber, m^2
b_i — Langmuir constant, min^{-1}
C_{bi} — Concentration of solute i in the fluid phase of the column, kg/m^3
c_{bi} — Scaled concentration of solute i in the fluid phase of the column C_{pi}/C_{oi}
C_e — Equilibrium concentration, mg/L
C_{oi} — Initial concentration of solute i, mg/L
C_{pi} — Concentration of solute i in the fluid phase within the pores of the zeolite, kg/m^3
c_{pi} — Scaled concentration of solute i in the fluid phase within the pores of the zeolite C_{pi}/C_{oi}
D_{pi} — Pore diffusion coefficient of component i, m^2/s
d_p — Particle diameter, m
K_{qt} — Life factor in Eq. (30), mg/g cycle
K_{tb} — Life factor in Eq. (31), h/cycle
k_{fi} — External mass transfer coefficient of solute i, m/s
L — Bed height, m
Q — Flow rate, L/s
q_e — Equilibrium zeolite capacity, mg/g
q_{mi} — Adsorption equilibrium constant defined by Langmuir equation of component i, mg/g
q_T — Zeolite capacity in packed bed, mg/g
q_{TI} — Initial zeolite capacity, mg/g
R — Radial distance in the particle, m
Re — Reynolds number, ρυdp/μw
R_p — Radius of particle, m
r — Scaled radial distance in the particle R/R_p
t — Time, s
t_e — Breakthrough time, s
t_b — Initial breakthrough time, s
V_0 — Initial solution volume, l
V_f — Final solution volume, l
W_A — Zeolite dosage, g

Greek symbols

ε_b — Bed porosity
ε_p — Particle porosity
υ — Interstitial velocity ($Q/A\varepsilon p$), m/s
ρ_p — Density of particle, kg/m^3
ρ_w — Density of water, kg/m^3
μ_w — Viscosity of water, Pa s

Subscripts

j — Integer value
L — Liquid phase
p — Pore phase

References

[1] P.H. Howard, Handbook of Environmental Fate and Exposure Data: For Organic Chemicals, Volume III Pesticides, CRC Press, Lewis Publishers, Inc., Chelsea, Michigan, 1991.
[2] R. Budd, A. O'Geen, K.S. Goh, S. Bondarenko, J. Gan, Efficacy of constructed wetlands in pesticide removal from tailwaters in the Central Valley, California, Environ. Sci. Technol., 43 (2009) 2925–2930.
[3] N. Stamatis, D. Hela, I. Konstantinou, Pesticide inputs from the sewage treatment plant of Agrinio to River Acheloos, western Greece: occurrence and removal, Water. Sci. Technol., 62 (2010) 1098–1105.
[4] G.Z. Memon, M. Bhanger, M. Akhtar, F.N. Talpur, J.R. Memon, Adsorption of methyl parathion pesticide from water using watermelon peels as a low cost adsorbent, Chem. Eng. J., 138 (2008) 616–621.
[5] M. Banaee, A. Mirvagefei, G. Rafei, B. Majazi Amiri, Effect of sub-lethal diazinon concentrations on blood plasma biochemistry, Int. J. Environ. Res., 2 (2008) 189–198.

[6] A.A. Amooey, S. Ghasemi, S.M. Mirsoleimani-azizi, Z. Gholaminezhad, M.J. Chaichi, Removal of Diazinon from aqueous solution by electrocoagulation process using aluminum electrodes, Korean J. Chem. Eng., 31 (2014) 1016–1020.
[7] L. Ezemonye, T. Ikpesu, I. Tongo, Distribution of diazinon in water, sediment and fish from Warri River, Niger Delta, Nigeria, Jordan J. Biol. Sci., 1 (2008) 77–83.
[8] A. Bermúdez-Couso, D. Fernández-Calviño, M. Pateiro-Moure, J.C. Nóvoa-Muñoz, J. Simal-Gándara, M. Arias-Estévez, Adsorption and desorption kinetics of carbofuran in acid soils, J. Hazard. Mater., 190 (2011) 159–167.
[9] Z. Aksu, E. Kabasakal, Batch adsorption of 2,4-dichlorophenoxy-acetic acid (2,4-D) from aqueous solution by granular activated carbon, Sep. Purif. Technol., 35 (2004) 223–240.
[10] M. Arienzo, M. Sanchez-Camazano, T.C. Herrero, M. Sanchez-Martin, Effect of organic cosolvents on adsorption of organophosphorus pesticides by soils, Chemosphere, 27 (1993) 1409–1417.
[11] A. Jonidi-Jafari, M. Shirzad-Siboni, J.-K. Yang, M. Naimi-Joubani, M. Farrokhi, Photocatalytic degradation of diazinon with illuminated ZnO–TiO_2 composite, J. Taiwan Inst. Chem. Eng., 50 (2015) 100–107.
[12] Y. Sun, J.J. Pignatello, Photochemical reactions involved in the total mineralization of 2,4-D by iron (3+)/hydrogen peroxide/UV, Environ. Sci. Technol., 27 (1993) 304–310.
[13] S. Salvestrini, P. Vanore, P. Iovino, V. Leone, S. Capasso, Adsorption of simazine and boscalid onto acid-activated natural clinoptilolite, Environ. Eng. Manage. J., 14 (2015) 1705–1712.
[14] S.N. Azizi, N. Asemi, Parameter optimization of the fungicide (Vapam) sorption onto soil modified with clinoptilolite by Taguchi method, J. Environ. Sci. Health., Part B, 45 (2010) 766–773.
[15] A. Shukla, Y.-H. Zhang, P. Dubey, J. Margrave, S.S. Shukla, The role of sawdust in the removal of unwanted materials from water, J. Hazard. Mater., 95 (2002) 137–152.
[16] Ş. Aslan, A. Türkman, Simultaneous biological removal of endosulfan (α+β) and nitrates from drinking waters using wheat straw as substrate, Environ. Int., 30 (2004) 449–455.
[17] R.E. Apreutesei, C. Catrinescu, C. Teodosiu, Studies regarding phenol and 4-chlorophenol sorption by surfactant modified zeolites, Environ. Eng. Manage. J., 8 (2009) 651–656.
[18] E. Iglesias-Jiménez, M. Sanchez-Martin, M. Sánchez-Camazano, Pesticide adsorption in a soil-water system in the presence of surfactants, Chemosphere, 32 (1996) 1771–1782.
[19] L. Nemeth-Konda, G. Füleky, G. Morovjan, P. Csokan, Sorption behaviour of acetochlor, atrazine, carbendazim, diazinon, imidacloprid and isoproturon on Hungarian agricultural soil, Chemosphere, 48 (2002) 545–552.
[20] J. Lemić, D. Kovačević, M. Tomašević-Čanović, D. Kovačević, T. Stanić, R. Pfend, Removal of atrazine, lindane and diazinone from water by organo-zeolites, Water Res., 40 (2006) 1079–1085.
[21] Z.B. Ouznadji, M.N. Sahmoune, N.Y. Mezenner, Adsorptive removal of diazinon: kinetic and equilibrium study, Desal. Wat. Treat., 57 (2016) 1880–1889.
[22] A. Rujiwatra, A selective preparation of phillipsite and sodalite from perlite, Mater. Lett., 58 (2004) 2012–2015.
[23] J. Cejka, A. Corma, S. Zones, Zeolites and Catalysis: Synthesis, Reactions and Applications, John Wiley & Sons, New York City, United States, 2010.
[24] S.K. Hassaninejad-Darzi, M. Rahimnejad, Electrocatalytic oxidation of methanol by ZSM-5 nanozeolite-modified carbon paste electrode in alkaline medium, J. Iran. Chem. Soc., 11 (2014) 1047–1056.
[25] L. Li, W. Li, C. Sun, L. Li, Fabrication of carbon paste electrode containing 1:12 phosphomolybdic anions encapsulated in modified mesoporous molecular sieve MCM-41 and its electrochemistry, Electroanalysis, 14 (2002) 368–375.
[26] J. Felsche, S. Luger, C. Baerlocher, Crystal structures of the hydro-sodalite $Na_6[AlSiO_4]_6$ $8H_2O$ and of the anhydrous sodalite $Na_6[AlSiO_4]_6$, Zeolites, 6 (1986) 367–372.
[27] N. Kalantari, M.J. Vaezi, M. Yadollahi, A.A. Babaluo, B. Bayati, A. Kazemzadeh, Synthesis of nanostructure hydroxy sodalite composite membranes via hydrothermal method: support surface modification and synthesis method effects, Asia-Pac. J. Chem. Eng., 10 (2015) 45–55.
[28] J.-C. Buhl, T.M. Gesing, C. Rüscher, Synthesis, crystal structure and thermal stability of tetrahydroborate sodalite $Na_8[AlSiO_4]_6(BH_4)_2$, Microporous Mesoporous Mater., 80 (2005) 57–63.
[29] M. Ogura, K. Morozumi, S. Elangovan, H. Tanada, H. Ando, T. Okubo, Potassium-doped sodalite: a tectoaluminosilicate for the catalytic material towards continuous combustion of carbonaceous matters, Appl. Catal. B, 77 (2008) 294–299.
[30] M. Armaghan, M.M. Amini, Adsorption of diazinon and fenitothion on MCM-41 and MCM-48 mesoporous silicas from non-polar solvent, Colloid J., 71 (2009) 583–588.
[31] R. Rostami, A.J. Jafari, Application of an adsorptive-thermocatalytic process for BTX removal from polluted air flow, J. Environ. Health. Sci. Eng., 12 (2014) 1–9.
[32] S.-S. Hong, G.-H. Lee, G.-D. Lee, Catalytic combustion of benzene over supported metal oxides catalysts, Korean J. Chem. Eng., 20 (2003) 440–444.
[33] J. Xiao, Y. Liu, J. Wang, P. Bénard, R. Chahine, Finite element simulation of heat and mass transfer in activated carbon hydrogen storage tank, Int. J. Heat Mass Transf., 55 (2012) 6864–6872.
[34] A.H. Sulaymon, S.A. Yousif, M.M. Al-Faize, Competitive biosorption of lead mercury chromium and arsenic ions onto activated sludge in fixed bed adsorber, J. Taiwan Inst. Chem. Eng., 45 (2014) 325–337.
[35] M.M. Treacy, J.B. Higgins, Collection of Simulated XRD Powder Patterns for Zeolites, 5th Ed. (Revised), Elsevier, Amsterdam, Netherlands, 2007.
[36] J.-C. Buhl, T.M. Gesing, T. Hoefs, C.H. Ruescher, Synthesis and crystal structure of gallosilicate-and aluminogermanate tetrahydroborate sodalites $Na_8[GaSiO_4]_6(BH_4)_2$ and $Na_8[AlGeO_4]_6(BH_4)_2$, J. Solid State Chem., 179 (2006) 3877–3882.
[37] D. Arieli, D. Vaughan, D. Goldfarb, New synthesis and insight into the structure of blue ultramarine pigments, J. Am. Chem. Soc., 126 (2004) 5776–5788.
[38] S.-R. Lee, M. Park, Y.-S. Han, J.-H. Choy, Solid–solid transformation route to nanocrystalline sodalite from Al-PILC at room temperature, J. Phys. Chem. Solids, 65 (2004) 421–424.
[39] S. Pourali, A. Samadi-Maybodi, Role of gel aging in template-free synthesis of micro and nano-crystalline sodalites, Chem. Solid Mater., 2 (2015) 21–31.
[40] T.-Z. Ren, Z.-Y. Yuan, B.-L. Su, Surfactant-assisted preparation of hollow microspheres of mesoporous TiO_2, Chem. Phys. Lett., 374 (2003) 170–175.
[41] S.C. Popescu, S. Thomson, R.F. Howe, Microspectroscopic studies of template interactions in $AlPO_4$-5 and SAPO-5 crystals, Phys. Chem. Chem. Phys., 3 (2001) 111–118.
[42] K.-H. Schnabel, G. Finger, J. Kornatowski, E. Löffler, C. Peuker, W. Pilz, Decomposition of template in SAPO-5 and $AlPO_4$-5 molecular sieves studied by IR and Raman spectroscopy, Microporous Mater., 11 (1997) 293–302.
[43] P. Gupta, A. Nanoti, M. Garg, A. Goswami, The removal of furfural from water by adsorption with polymeric resins, Sep. Sci. Technol., 36 (2001) 2835–2844.
[44] E. Wilson, C. Geankoplis, Liquid mass transfer at very low Reynolds numbers in packed beds, Ind. Eng. Chem. Fundam., 5 (1966) 9–14.
[45] D.W. Hand, J.C. Crittenden, W.E. Thacker, User-oriented batch reactor solutions to the homogeneous surface diffusion model, J. Environ. Eng., 109 (1983) 82–101.
[46] H. Esfandian, H. Javadian, M. Parvini, B. Khoshandam, R. Katal, Batch and column removal of copper by modified brown algae sargassum bevanom from aqueous solution, Asia-Pac. J. Chem. Eng., 8 (2013) 665–678.
[47] I.A. Aguayo-Villarreal, A. Bonilla-Petriciolet, V. Hernández-Montoya, M.A. Montes-Morán, H.E. Reynel-Avila, Batch and column studies of Zn^{2+} removal from aqueous solution using chicken feathers as sorbents, Chem. Eng. J., 167 (2011) 67–76.
[48] K. Vijayaraghavan, J. Jegan, K. Palanivelu, M. Velan, Biosorption of copper, cobalt and nickel by marine green alga *Ulva reticulata* in a packed column, Chemosphere, 60 (2005) 419–426.